Biochimica et Biophysica Acta, 1106 (1992) 242–250

BBAMEM 75629

Interdigitated bilayer packing motifs: Raman spectroscopic studies of the eutectic phase behavior of the 1-stearoyl-2-caprylphosphatidylcholine/dimyristoylphosphatidylcholine binary mixture

James L. Slater [a], Ching-hsien Huang [b] and Ira W. Levin [a]

[a] *Laboratory of Chemical Physics, National Institute of Diabetes and Digestive and Kidney Diseases, National Institutes of Health, Bethesda, MD (USA) and* [b] *Department of Biochemistry, University of Virginia Health Sciences Center, Charlottesville, VA (USA)*

(Received 22 October 1991)

Key words: Raman spectroscopy; Phospholipid binary mixture; Eutectic phase behavior; 1-Stearoyl-2-caprylphosphatidylcholine; Dimyristoylphosphatidylcholine; Mixed interdigitated bilayer

The thermotropic properties and acyl chain packing characteristics of multilamellar dispersions of binary mixtures of 1-stearoyl-2-caprylphosphatidylcholine (C(18):C(10)PC), an asymmetric chain species, and dimyristoylphosphatidylcholine (C(14):C(14)PC), a symmetric chain lipid, were monitored by vibrational Raman spectroscopy. In order to examine each component of the binary mixture separately, the acyl chains of the symmetric chain species were perdeuterated. As shown by differential scanning calorimetry, the mismatch in the gel phase bilayer thickness between the two lipid components generates a lateral phase separation resulting in two distinct gel phases, G(I) and G(II), which coexist over much of the composition range. The Raman data demonstrate that the *mixed interdigitated* phase (three chains per headgroup), analogous to single component phase behavior, is retained when the C(18):C(10)PC component act as a host for the G(I) gel phase. In contrast, the C(18):C(10)PC molecules exhibit *partial interdigitation* (two chains per headgroup) when they are included as guests within the C(14):C(14)PC host matrix to form the G(II) gel phase. Compared to pure C(14):C(14)PC bilayers at equivalent reduced temperatures, the host G(II) gel phase C(14):C(14)PC molecules exhibit an increased acyl chain order, while for the host G(I) gel phase the C(14):C(14)PC lipid species show increased intrachain disorder.

Introduction

Since the initial discussions of an interdigitated chain structure for a dipalmitoylphosphatidylglycerol bilayer [1], much interest has been generated, particularly in recent years, by model system studies of interdigitated single, symmetric and asymmetric chain systems (for review, see Refs. 2–4). In addition to studies of pure bilayer species, examinations of multicomponent systems have contributed toward clarifying the balance of forces governing specific interdigitated membrane forms. For example, differential scanning calorimetric, X-ray diffraction and Raman spectroscopic techniques were used to examine the formation of domains and mixing properties of completely interdigitated dihexadecylphosphatidylcholine, a symmetric chain lipid, in conventional bilayers of dipalmitoylphosphatidylcholine [5–7]. In other two-component systems involving asymmetric chain lipids, the long acyl chains of glycosphingolipids, occurring as minor components in bilayers, have been shown by deuterium magnetic resonance and electron spin resonance spectroscopies to penetrate the opposing monolayer of a bilayer matrix [8,9].

In the present study, we present a vibrational Raman spectroscopic study which extends previous investigations of highly asymmetric chain lipid species by stressing the bilayer interactions and phase behavior of the binary mixture of 1-stearoyl-2-caprylphosphatidylcholine ((C(18):C(10)PC)) and dimyristoylphosphatidylcholine ((C(14):C(14)PC)), lipids representative of asymmetric and symmetric chain systems, respectively. The thermal properties and phase diagram of this novel lipid mixture have been previously elucidated by Lin and Huang [10] using differential scanning calorimetric methods. Specific interest in the C(18):C(10)PC species, whose *sn*-1 acyl chain is nearly twice the length of the *sn*-2 chain moiety, stems from the observation that fully hydrated dispersions of this lipid undergo a gel to liquid-crystalline phase transition in which the

Correspondence: I.W. Levin, NIDDK, National Institutes of Health, Bethesda, MD 20892, USA.

mixed interdigitated gel phase structure, characterized by three acyl chain cross sectional areas subtended by a single headgroup area, transforms directly to the partially interdigitated fluid phase [11–13]. The latter phase reflects a structure in which only two chain areas are circumscribed by the headgroup. Since symmetric chain systems, represented by C(14):C(14)PC in the binary mixture, do not form interdigitated bilayers except under high pressure [14,15] or by the addition of specific aqueous phase mediators [3], an opportunity arises for deriving from spectroscopic considerations a detailed molecular interpretation of the packing of requirements of a binary lipid mixture which exhibits widely variant gel phase structural properties and eutectic phase behavior.

Raman spectroscopy offers several advantages in studying bilayer chain interdigitation relative to other spectroscopic techniques. First, a wealth of vibrational information is derived noninvasively; that is, no probe molecules which may perturb either the hydrocarbon region of the bilayer or the organization of the interstitial water between bilayers are introduced. Second, by perdeuteration of the hydrocarbon chains of one of the components of the binary mixture, the bilayer behavior of each lipid species can be separately monitored as a function of temperature and mole fraction of the mixture. This is a critical aspect of the present investigation, since only slight changes occur in the overall membrane order of the C(18):C(10)PC/C(14):C(14)PC bilayer mixture despite the manifestation of highly variable structural features of the components within each bilayer phase. We emphasize that these individual structural differences are not easily determined by techniques providing only the overall order of the binary system.

Materials and Methods

C(18):C(10)PC was synthesized as previously described [16,17]. DMPC and DMPC-d_{54} was purchased from Avanti Polar Lipids. Two component systems were prepared in the following manner. Chloroform solutions of the individual components were thoroughly mixed, and excess solvent was removed by evaporation with a stream of nitrogen prior to placing under high vacuum for several hours. These samples were then dissolved together in a minimal amount of benzene and lyophilized overnight under high vacuum. Lyophilized samples were hydrated in 50 mM KCl by vortexing and by repeated passage through the phase transition. The hydrated samples were then placed in a capillary tube and pelleted using a microcapillary centrifuge.

Raman spectroscopy was performed using the 514.5 nm exciting line of an Innova 100 argon ion laser with excitation power levels of 200 mW at the sample. Variation of laser intensity levels between 125 and 400 mW demonstrated that under the conditions of the present experiments no significant laser heating effects of the bilayer arose. Spectra were collected at a spectral resolution of 5 cm^{-1} on a Spex Ramalog 6 spectrometer equipped with holographic gratings. The monochrometer was calibrated utilizing atomic argon lines; vibrational frequencies, when required, are determined to ± 2 cm^{-1}. Temperature control was accurate to ± 0.1 degrees. Data were collected on a microcomputer based system and passed to a Sun Unix fileserver for storage and analysis using software developed at the National Institutes of Health.

Generally, 5 to 10 spectra were signal averaged in the C-H and C-D spectral regions prior to determining the various peak intensity ratios for constructing the temperature profiles. The errors associated with intensity ratios from individual spectra are less than ± 0.02 [18]. Data representing order parameters as a function of temperature were fit to a two state model of the phase transition in order to determine the bilayer transition temperature T_m and transition width ΔT, as well as lipid interchain and intrachain order parameters before and after the phase transition [19]. When the acyl chain carbon-hydrogen (C-H) stretching mode region of the nondeuterated component is examined in binary systems with deuterated chain components, contributions to the C-H stretching mode region arise from the unlabelled headgroup moiety of the deuterated chain lipids. The necessary corrections are made to the C-H stretching mode region of the unlabeled species by renormalizing and subtracting the spectra originating from the C-H stretching mode region of the deuterated component.

Results

Representative Raman spectra reflecting the acyl chain methyl and methylene 2900 cm^{-1} carbon-hydrogen (C-H) and 2100 cm^{-1} carbon deuterium (C-D) stretching mode region are shown in Figs. 1A and B, respectively, for aqueous dispersions of the binary mixture at its eutectic composition; namely, 60 mol% C(18):C(10)PC and 40 mol% C(14):C(14)PC. Various peak height intensity ratios have been described for deriving the thermal characteristics of membrane bilayers in terms of hydrocarbon chain intermolecular (chain-chain) and intramolecular (*trans/gauche*) interactions [18,20]. The vibrational assignments and dynamics in terms of the methyl and methylene stretching modes, coupled oscillator and Fermi resonance effects upon which these intensity ratios are based, have been discussed in detail (see, for example, Ref. 20 and references contained therein). For example, in the C-H stretching mode region the I_{2935}/I_{2880} peak height intensity ratio, which involves spectral features reflecting

the terminal chain methyl symmetric C-H stretching modes and the methylene asymmetric C-H stretching modes, provides a parameter reflecting the superposition of *trans/gauche* conformational rearrangements upon lateral chain-chain order/disorder characteristics. The complimentary I_{2850}/I_{2880} intensity ratio, representing features originating from the hydrocarbon chain methylene C-H symmetric and asymmetric stretching modes, respectively, describe primarily lipid interchain interactions. These ratios are defined such that they scale with increasing bilayer disorder.

Interchain and intrachain processes are also determined from the 2200 cm^{-1} C-D stretching mode region. Detailed vibrational assignments for this spectral interval have also been discussed previously [18]. In particular, the I_{2177}/I_{2076} peak height intensity ratio reflects intermolecular order/disorder effects, while the I_{2177}/I_{2103} index monitors intrachain order/disorder changes primarily in the distal portion of the acyl chain near the methyl terminus [18]. The additional I_{2197}/I_{2103} and I_{2197}/I_{2076} ratios characterize primarily intrachain effects in the proximal portion of the acyl chain near the polar/apolar interface.

Temperature dependent profiles, derived from the

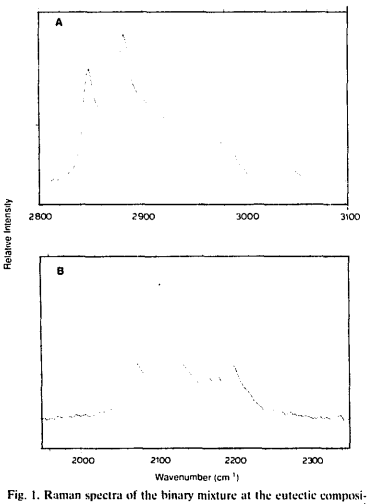

Fig. 1. Raman spectra of the binary mixture at the eutectic composition 60% C(18):C(10)PC/40% C(14):C(14)PC-d_{54}. (A) 2900 cm^{-1} C-H stretching mode region. (B) 2100 cm^{-1} C-D stretching mode region.

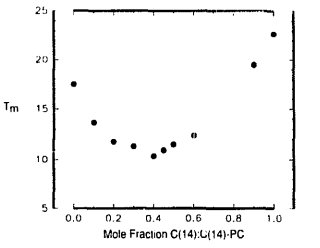

Fig. 2. Phase transition temperatures for the binary system C(18):C(10)PC/C(14):C(14)PC as a function of the mole fraction of C(14):C(14)PC. Transition midpoint temperatures were determined from I_{2935}/I_{2880} peak height intensity ratio of the 2900 cm^{-1} spectral region representing a superposition of the acyl chain C-H stretching modes of both lipid species. The melting point depression at 40 mol% C(14):C(14)PC/60 mol% C(18):C(10)PC is characteristic of a eutectic point for this system.

various order-disorder parameters and fit to a two-state statistical mechanical model [19], provide values for the phase transition midpoint temperature (T_m) of a given sample and allow comparisons of bilayer packing characteristics within the gel and liquid-crystalline phases, respectively. Fig. 2 presents a plot of these T_m's determined from temperature profiles of the I_{2935}/I_{2880} intensity ratio as a function of composition for the binary C(18):C(10)PC/C(14):C(14)PC system in which neither component is deuterated. Thus, the ratio represents a property of the entire bilayer since both lipid components of the binary mixture contribute to the C-H stretching mode region. A remarkable feature of these mixtures is that all exhibit lower values of T_m than the T_m of either pure component. The observed behavior for the melting point depressions are characteristic of a eutectic system [10,21]. This eutectic point minimum at 10.4°C, corresponding to a sample of 40 mol% C(14):C(14)PC and 60 mol% C(18):C(10)PC, is in good agreement with previous high sensitivity differential scanning calorimetry results [10]. Although the T_m's derived from the Raman data for the various mole fractions of the binary mixture are, in general, slightly lower than the calorimetric data, we do not believe that the spectroscopic results arise solely from localized laser heating effects (see Materials and Methods) but may also originate from kinetic effects implicit in the long incubation times required for obtaining the vibrational spectra. (That is, laser excitation power levels varying from about 125 to 400 mW failed to influence the reproducibility in the measured values of T_m). Table I summarizes the T_m and ΔT data obtained for the C(18):C(10)PC/C(14):C14)PC system from the vibrational data.

TABLE I

Summary of the transition temperatures (T_m) and transition widths (ΔT) for binary mixtures of C(18):C(10)PC/C(14):C(14)PC

Transition temperatures T_m and transition widths ΔT were determined from temperature profiles constructed from Raman spectral data I_{2935}/I_{2880} derived from the C-H stretching mode region. The intensity ratios were fit to a two-state statistical mechanical model [19].

Mole fraction C(14):C(14)PC	T_m (°C)	ΔT in (C°)
0	17.5±0.1	0.3±0.1
0.10	13.7±0.1	1.7±0.1
0.20	11.8±0.1	2.9±0.1
0.30	11.3±0.1	1.2±0.1
0.40	10.4±0.1	0.9±0.1
0.45	11.0±0.1	0.9±0.1
0.50	11.5±0.1	1.0±0.1
0.60	12.4±0.1	3.2±0.1
0.70	19.5±0.1	1.7±0.1
1.00	22.7±0.1	1.3±0.1

In order to assess the relative values of the global interchain and intrachain order/disorder parameters about the phase transition temperature of a given lipid mixture, we present the Raman temperature profile data in terms of a common reduced temperature above and below T_m as a function of the composition variable. Figs. 3A and B show values of two peak height intensity ratios, I_{2935}/I_{2880} and I_{2850}/I_{2880}, respectively, plotted against mole fraction C(14):C(14)PC at reduced temperatures (T_{red}) both below and above the phase transition temperature ($T_{red} = \pm 0.02$, approximately ±6°C). Below the phase transition temperature, beginning with pure C(18):C(10)PC and with increasing mol% of C(14):C(14)PC, we observe a relatively constant order reflected by the I_{2935}/I_{2880} parameter towards 20 mol% C(14):C(14)PC, followed by a smooth, continuous increase in disorder for increasing concentrations of the symmetric chain species as the value of the order parameter for pure C(14):C(14)PC bilayers is approached (Fig. 3A). In contrast, the I_{2850}/I_{2880} parameter, reflecting primarily interchain order, appears first to increase from 0 to 20 mol% with increasing C(14):(14)PC, then decreases to the eutectic point at 0.4 mol% C(14):C(14)PC, and then finally increases, continuously toward the value of the order exhibited by pure C(14):C(14)PC bilayers (Fig. 3B). Although we estimate the errors in the intensity ratios to be less than ±0.02 [18], the trends noted in the order/disorder parameters are reproducible for points within the margins of overlap. Above the phase transition temperature, as C(14):C(14)PC is added to C(18):C(10)PC, we observe an increase in the interchain I_{2850}/I_{2880} parameter as 30 mol% C(14):C(14)PC is approached. A decrease in disorder occurs upon further increase in the mole fraction of C(14):C(14)PC (Fig. 3B). Similarly, above the phase transition, the superposition of the intrachain and interchain order reflected in the I_{2935}/I_{2880} parameter appears remarkably constant between 0 and 50 mol% C(14):C(14)PC; the discontinuity which appears between 50 and 60 mol% is followed by a rise towards the value associated with pure C(14):C(14)PC bilayers (Fig. 3A).

By focusing attention on the temperature profiles derived from the I_{2935}/I_{2880} and I_{2850}/I_{2880} order/disorder parameters for the two pure components and the eutectic composition (Figs. 4A and 4B), several generalization become apparent. As noted in previous Raman spectroscopic studies [11] and in Figs. 4A and B, pure C(18):C(10)PC bilayers, which undergo a transition from the mixed interdigitated gel to the partially interdigitated fluid phase, exhibit greater intermolecular and intramolecular order below the phase transition relative to pure C(14):C(14)PC bilayers. Below the phase transition, the gel phase eutectic composi-

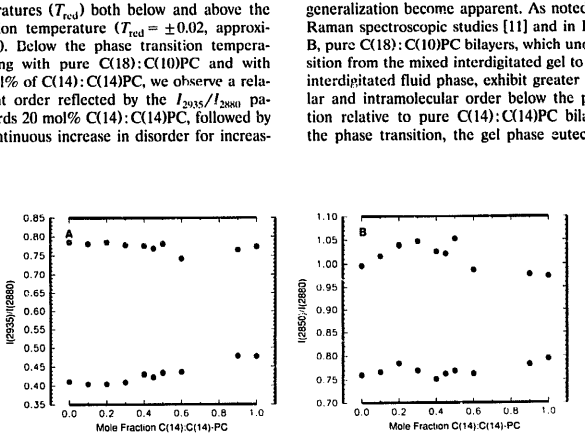

Fig. 3. Peak height intensity ratios: (A) I_{2935}/I_{2880} and (B) I_{2850}/I_{2880}, as a function of the mole fraction of C(14):C(14)PC. Intensity ratios are taken at a reduced temperature $T_{red} = \pm 0.02$ (approximately ±6°C) about the phase transition temperatures. The errors in the intensity ratios are less than ±0.02.

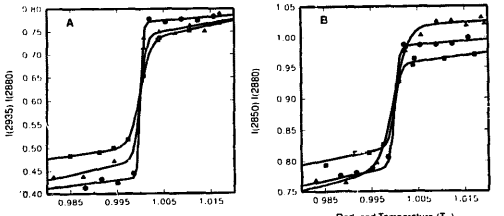

Fig. 4. Temperature profiles determined from peak height intensity ratios: (A) I_{2935}/I_{2880} and (B) I_{2850}/I_{2880}, as a function of reduced temperature for C(18):C(10)PC (●), 60% C(18):C(10)PC/40% C(14):C(14)PC (the eutectic composition); (▲) C(14):C(14)PC (■). The intensity ratio derived from the 2900 cm^{-1} spectral region for the eutectic composition represents a superposition of the acyl chain C-H stretching modes of both lipid species.

tion displays intermolecular order similar to pure C(18):C(10)PC (Fig. 4B). Above the phase transition, the eutectic composition exhibits greater intermolecular disorder than either of the pure components (Fig. 4B). Again, the data in these figures for the eutectic composition represent global order/disorder parameters since both bilayer components contain normal, hydrogenated acyl chains.

At this point, our strategy is to describe the specific phase behavior of each component by determining Raman spectra associated with binary systems composed of hydrogenated C(18):C(10)PC chain species (represented by C(18):C(10)PC-d_0) in association with perdeuterated chain (C(14):C(14)PC species (represented by C(14):C(14)PC-d_{54}), remembering that chain deuteration results only in an isomorphous replacement [22]. Thus, the structural properties of the C(18):C(10)PC component in the mixture are determined from the 2900 cm^{-1} C-H stretching mode region spectra, while the packing characteristics of the C(14):C(14)PC-d_{54} species are derived from the analogous 2100 cm^{-1} C-D stretching mode region reflecting the deuterated methylene groups.

Fig. 5 displays for several binary compositions the gel phase intensity ratios, corrected for the headgroup contributions from the perdeuterated species, of the I_{2935}/I_{2880} and I_{2850}/I_{2880} order/disorder parameters for C(18):C(10)PC-d_0 at a common reduced temperature (−6°C) below the phase transition T_m. These gel phase values thus reflect the relative interchain and intrachain order possessed by C(18):C(10)PC at each of four compositions. In the phase diagram established for this binary eutectic system [10], the G(I) gel phase exists in a single phase region between 0 and about 20 mol% C(14):C(14)PC, while the G(II) gel phase exists in a single phase region between approx. 75 and 100 mol% C(14):C(14)PC; these two gel phases coexist in equilibrium in a two phase region between 20 and 75 mol% C(14):C(14)PC [10]. The intermolecular gel phase disorder, measured by the I_{2850}/I_{2880} parameter in the figure, increases monotonically, but quite gradually, as C(14):C(14)PC-d_{54} is added to the mixture. We note, however, that the same trend is not indicated for the I_{2935}/I_{2880} order/disorder parameter, which contains contributions from both intramolecular and intermolecular interactions. This ratio increases, indicating greater bilayer disorder, only when the predominent environment for C(18):C(10)PC is the G(II) gel phase (20 mol% (C(18):C(10) PC/80 mol% (C(14):C(14)PC-d_{54}). This increased disorder relative to pure C(18):C(10)PC bilayers is consistent with G(18):C(10)PC guest molecules exhibiting partial interdigitation in the G(II) phase. That is, the partially interdigitated phase displays a greater disorder than the mixed interdigi-

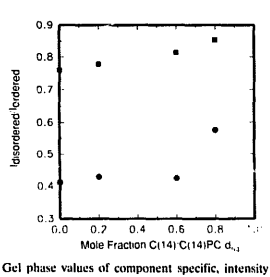

Fig. 5. Gel phase values of component specific, intensity corrected order/disorder parameters for the binary system C(18):C(10)PC-d_0/C(14):C(14)PC-d_{54} taken at a common reduced temperature (6°C below the respective phase transition temperature). ●, I_{2935}/I_{2880}; ■, I_{2850}/I_{2880}.

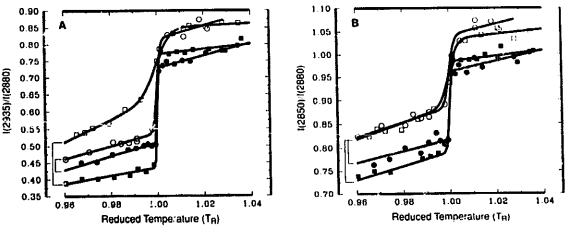

Fig. 6. Temperature profiles constructed from (A) I_{2935}/I_{2880} and (B) I_{2850}/I_{2880} intensity ratios for C(18):C(10)PC-d_0 (■), C(14):C(14)PC-d_0 (●), 20% C(14):C(14)PC-d_0/80% C(14):C(14)PC-d_{54} (○), and 20% C(18):C(10)PC-d_0/80% C(14):C(14)PC-d_{54} (□). For ease in comparing profiles, the brackets associate changes expected for the dilution of C(14):C(14)PC-d_0 in C(14):C(14)PC-d_{54} (curves ● and ○) and changes expected for the lateral chain effects between pure C(18):C(10)PC-d_0 bilayers and C(18):C(10)PC-d_0 diluted by C(14):C(14)PC-d_{54} (curves ■ and □), respectively.

tated phase [11,23]. In the G(I) gel phase, the addition of increasing amounts of C(14):C(14)PC-d_{54} guest molecules to the C(18):C(10)PC host matrix does not result in a substantial increase in the disorder of the host matrix, which we interpret as maintaining a constant intramolecular (*trans/gauche*) order for the G(I) gel phase.

In isotopically diluting C(18):C(10)PC-d_0 with C(14):C(14)PC-d_{54}, matrix effects may perturb the I_{2935}/I_{2880} and I_{2850}/I_{2880} values by altering the lateral interactions between identical species. We assess these effects on the peak height intensity parameters by comparing temperature profiles of C(18):C(10)PC-d_0 diluted in a matrix of C(14):C(14)PC-d_{54} to a sample of C(14):C(14)PC-d_0 diluted in a matrix of C(14):C(14)PC-d_{54}. These comparisons, shown in Figs. 6A and B for pure C(18):C(10)PC-d_0 and C(14):C(14)PC-d_0 bilayers and for 20% C(14):C(14)PC-d_0/80% C(14):C(14)PC-d_{54} and 20% C(18):C(10)PC-d_0/80% C(14):C(14)PC-d_{54} bilayers, indicate that the increase in I_{2935}/I_{2880} and I_{2850}/I_{2880} order/disorder parameters for C(18):C(10)PC in the G(II) gel phase is not simply a consequence of changes in the lateral Fermi resonance interactions between like chains. As displayed in Fig. 6A for the gel phase I_{2935}/I_{2880} index, pure samples of C(18):C(10)PC-d_0 are significantly more ordered than C(14):C(14)PC-d_0 bilayers. Dilution of the C(14):C(14)PC-d_0 matrix with 80 mol% C(14):C(14)PC-d_{54} results in only a slight change in the I_{2935}/I_{2850} ratios. This alteration in intensity is attributed to a rearrangement of the C-H stretching mode intensities as a consequence of the perturbation to the lateral interactions of like chains. Dramatic changes occur in the gel phase I_{2935}/I_{2880} ratios for the bilayers comprised of 20% C(18):C(10)PC and 80% C(14):C(14)PC-d_{54} in that the temperature profile for the bilayer is characteristic of a significant gel phase disorder coupled to a broadened gel to liquid-crystalline phase transition. That is, the additional increase in these order/disorder parameters must result from the change in the gel phase packing properties as the system passes from a mixed interdigitation state in the pure C(18):C(10)PC bilayer to the partial interdigitation arrangement characteristic of the C(18):C(10)PC in the G(II) gel phase of the binary system. Note the similarity of the intermolecular order described by the I_{2850}/I_{2880} indices between the matrix diluted C(14):C(14)PC-d_0 and the matrix diluted C(18):C(10)PC-d_0 bilayer samples (Fig. 6B). These data provide additional support for a model of partial interdigitation of the C(18):C(10)PC component within the G(II) gel phase in which a partially interdigitated C(18):C(10)PC species (two chains per headgroup) exhibits greater gel phase disorder than a mixed interdigitated species (three chains per headgroup).

Structural properties of the C(14):C(14)PC-d_{54} component of the various binary systems are examined independently by measurements derived from the 2100 cm^{-1} C-D stretching mode region of the Raman spectrum (Figs. 7A-D). The plots show that values of the order/disorder intensity ratios for the symmetric chain species, which increase for increasing bilayer disorder, increase, in general, as a function of bilayer matrix dilution. As discussed above, the I_{2177}/I_{2076} intensity ratio monitors primarily interchain interactions, while the I_{2177}/I_{2103} ratio monitors primarily intrachain interactions of the lipid chains near the methyl termini of the acyl chains [18]. The I_{2197}/I_{2103} and I_{2197}/I_{2076} ratios probe primarily intrachain interactions of the lipid chains near the polar/apolar interface region [18]. To facilitate comparisons, values for the various order/disorder parameters taken below and above the

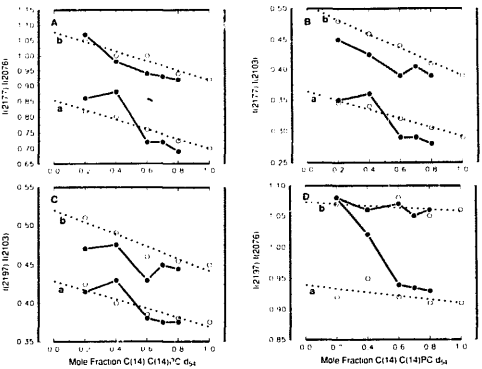

Fig. 7. Indices from the C-D stretching mode region for the binary system C(18):C(10)PC-d_0/C(14):C(14)PC-d_{54} (●) compared to C(14):C(14)PC-d_0/C(14):C(14)PC-d_{54} bilayers (○) determined below and above the corresponding phase transition temperatures at a common reduced temperature $T_{red} = \pm 0.02$: (A) I_{2177}/I_{2076}, (B) I_{2177}/I_{2103}, (C) I_{2197}/I_{2103}, (D) I_{2197}/I_{2076}.

phase transition at common reduced temperatures, $T_{red} = \pm 0.02$, are plotted as a function of the binary system composition. The C(14):C(14)PC-d_{54} guest molecules associated with the G(I) gel phase of the C(18): C(10)PC-d_0/C(14):C(14)PC-d_{54} binary mixture (Fig. 7Aa; 20 and 40 mol% C(14):C(14)PC-d_{54}) exhibit greater gel phase intermolecular disorder in comparison to the C(14):C(14)PC-d_0/C(14):C(14)PC-d_{54} bilayers at these mole fractions. In contrast, C(14): C(14)PC-d_{54} associated with the G(II) gel phase of the binary mixture (Fig. 7Aa; 60, 70 and 80 mol% C(14): C(14)PC-d_{54}) shows an increased intermolecular order in comparison to the C(14):C(14)PC-d_c/C(14): C(14)PC-d_{54} bilayer mixtures. Below the phase transition temperature, increased intramolecular ordering of the C(14):C(14)PC-d_{54} molecules within the G(II) gel phase of the C(18):C(10)PC-d_0/C(14):C(14)PC-d_{54} mixture is observed for the distal portion of the C(14):C(14)PC-d_{54} acyl chains near the methyl termini (Fig. 7Ba; 60, 70 and 80 mol%) in comparison to the behavior of C(14):C(14)PC-d_0/C(14):C(14)PC-d_{54} bilayers.

C(14):C(14)PC-d_{54} at or near the eutectic composition of the C(18):C(10)PC-d_0/C(14):C(14)PC-d_{54} binary mixture exhibits the greatest amount of gel phase disorder relative to C(14):C(14)PC-d_0/C(14): C(14)PC-d_{54} bilayers (Figs. 7Aa–Da; 40 mol% C(14): C(14)PC-d_{54}). In the comparisons between the two types of binary mixtures, the proximal portion of the acyl chain (nearest to the ester linkage) in the G(I) phase remains disordered below the phase transition temperature (Fig. 7Da; 20 and 40 mol%). Above the phase transition, the general trend for the curves (Figs. 7Ab–Db) is that C(14):C(14)PC-d_{54} in the binary system with C(18):C(10)PC-d_0 exhibits equal or greater order in comparison with the C(14):C(14)PC-d_0/ C(14):C(14)PC-d_{54} bilayers.

Discussion

Both differential scanning calorimetry [10] and vibrational Raman spectroscopy indicate eutectic phase behavior for binary mixtures of C(18):C(10)PC and C(14):C(14)PC bilayers, two diacyl phosphoglycerides representative of highly asymmetric and symmetric chain phospholipids with the same total number of methylene units, respectively. Since vibrational Raman spectroscopy provides parameters delineating acyl chain packing arrangements, as well as the inherent intramolecular and intermolecular order of the hydrocarbon region of the bilayer matrix, the spectral data allow a detailed structural interpretation to be presented for the packing motifs assumed by the mixing of two disparate lipid species. The contribution of each lipid species to the domain structure of the bilayer mixture is assessed by deuterating the hydrocarbon chains of the symmetric chain lipid and then monitoring separately the temperature behavior of each lipid component. The domain and phase behavior of this class of binary mixtures is particularly relevant in understanding the membrane packing characteristics of more complex, asymmetric chain biological lipids in

which highly asymmetric lipid chains coexist with neighboring symmetric chain lipids.

The phase diagram for the C(18):C(10)PC/C(14):C(14)PC binary mixture, which was determined calorimetrically [10], shows three gel phase regions, the C(18):C(10)PC and C(14):C(14)PC enriched G(I) and G(II) regions, respectively, and the G(I) + G(II) two phase region. Although the acyl chains of C(18):C(10)PC and C(14):C(14)PC molecules contain the same number of methylene segments, the thickness of C(18):C(10)PC mixed interdigitated (three chains per headgroup) gel phase bilayers (33 Å at 10°C [12]) is significantly less than C(14):C(14)PC gel phase systems (43 Å at 10°C [24]). The ensuing bilayer mismatch of these two components results in the partial miscibility of the gel phase of these two species, although a match in bilayer thickness is restored for the liquid-crystalline phase in which the two components become completely miscible in all proportions. This limited gel phase miscibility, coupled with the ability to mix completely in the fluid phase, results in the characteristic eutectic behavior of the system.

The various hydrocarbon order parameters for both the $-d_0$ and $-d_{54}$ chains systems indicate that the hydrocarbon chains of C(18):C(10)PC are packed in the G(I) gel phase with mixed interdigitation, bearing three chains per headgroup. Fig. 5 shows that as the mole fraction of the C(14):C(14)PC-d_{54} component increases in mol% from 0 to 80, no perturbation occurs in the I_{2935}/I_{2850} parameter reflecting that the C(18):C(10)PC-d_0 species, which contains a superposition of intrachain (*trans/gauche* isomerization) and interchain effects is most likely packed in the mixed interdigitated form. A slight increase, however, is observed in the pure chain-chain I_{2850}/I_{2880} interaction parameter. Thus, through this mole fraction range, but particularly to the boundary of the G(I) + G(II) phase at 0.2 mole fraction of C(14):C(14)PC-d_{54}, the C(18):C(10)PC asymmetric chains remain in the mixed interdigitated configuration. The two C(14):C(14)PC-d_{54} parameters I_{2197}/I_{2076} and I_{2177}/I_{2076}, which reflect changes both in intrachain order in regions of the acyl chain close to the bilayer headgroup/interface area and in interchain interactions in portions of the chains near the methyl termini (Figs. 7Aa, Da), indicate that relative to its pure gel phase bilayer order, the symmetric chain species undergoes a chain disordering process. This rearrangement in C(14):C(14)PC-d_{54} order/disorder parameters enables the symmetric chain phospholipid molecule to be accommodated by the C(18):C(10)PC chain lattice. The intramolecular I_{2197}/I_{2076} index (Fig. 7Da) suggests that near the G(I) − G(I) + G(II) phase boundary the C(14):C(14)PC-d_{54} species achieves a chain disorder near the headgroup that is comparable to fluid phase characteristics.

The G(II) gel phase consists largely of a C(14):C(14)PC host matrix enriched with C(18):C(10)PC, which exists in the partially (two chains per headgroup) interdigitated state. The increase in gel phase disorder for the C(18):C(10)PC chains as a function of increasing mole fraction C(14):C(14)PC-d_{54} in the G(II) phase (Figs. 5 and 6) is consistent with the asymmetric chain species assuming an interdigitated form accommodating two chains per headgroup [11]. In order for the C(14):C(14)PC chains to maximize their van der Waals interactions with neighboring C(18):C(10)PC and C(14):C(14)PC chains, the tilt angle of the symmetric chain lipids would either be reduced or eliminated. Increased chain–chain interactions and increased *trans/gauche* conformer ratios within the C(14):C(14)PC-d_{54} lattice for mole fractions of C(14):C(14)PC-d_{54}, corresponding to the G(I) + G(II) and G(II) phases of the binary mixture [10], are observed for the symmetric chain species order/disorder parameters in Figs. 7Aa, Ba, and Ca.

The additional G(II) phase bilayer ordering for the symmetric chain lipid species, indicated by the I_{2177}/I_{2076} and I_{2177}/I_{2103} perdeuterated chain order/disorder parameters in Figs. 7Aa and 7Ba, may also be clarified by a structural argument based on the placement of the acyl chain methyl termini at varying bilayer depths. When C(18):C(10)PC is packed in the mixed interdigitated G(I) phase with C(14):C(14)PC, the terminal methyl groups of the *sn*-2 C(10) chain lie approximately at the bilayer midplane defined ordinarily by the methyl termini of symmetric chain lipid species. The terminal methyl group of the *sn*-1 C(18) chain, which penetrates the bilayer midplane, resides, however, near the bilayer polar/hydrophobic region interface. In contrast, the chain terminal methyl groups of C(18):C(10)PC in the partially interdigitated G(II) gel phase define along with the C(14):C(14)PC methyl termini, three distinct bilayer planes rather than the more narrowly located, conventional disordered bilayer center area. Without a well-defined bilayer midplane with its locus of chain disorder, one expects a significant reduction of the mobility of the terminal methyl groups of the symmetric chain C(14):C(14)PC species. The intra- and intermolecular ordering effects at the chain terminal regions, reflected by the I_{2177}/I_{2103} and I_{2177}/I_{2076} indices, respectively, are consistent with this prediction. Figs. 7A and B indicate that the chain ordering effects of C(14):C(14)PC-d_{54} are retained at concentrations corresponding to a single nearest neighbor of C(18):C(10)PC in the C(14):C(14)PC matrix.

Table I shows that local maxima in the phase transition cooperativities, reflected by a small value of ΔT, occur for both of the pure components of the C(18):C(10)PC-d_0/C(14):C(14)PC-d_0 binary mixture. These phase transition cooperativities are inversely related to the transition widths which are determined from the differences between the onset and completion

temperatures that are derived from the fit of the temperature dependent Raman I_{2935}/I_{2880} intensity data to a two-state model [19]. Although the C(14):C(14)PC lattice is significantly disordered near the eutectic composition (Fig. 7), the eutectic point also corresponds to a local maximum in transition cooperativity, or a minimum in transition width, as found in the calorimetric studies [11]. At the eutectic point, a given C(14):C(14)PC molecule may be nearest neighbors with either mixed interdigitated gel phase C(18):C(10)PC or partially interdigitated gel phase C(18):C(10)PC, since both the G(I) and G(II) gel phases coexist at this composition. If the C(14):C(14)PC molecules adopt sufficient intramolecular (*trans/gauche*) disorder and adjust to a bilayer thickness intermediate between these two different types of C(18):C(10)PC interdigitated acyl chain gel phase packing arrangements, then the sharp discontinuities arising from a mismatch in adjoining domains of G(I) and G(II) gel phase regions are avoided. Coexistence of the G(I) and G(II) gel phase domains in this two phase region of the phase diagram (between 20 and 75 mol% below the eutectic horizontal), may be accomplished in this packing arrangement without a requirement for the 'interfacial' or boundary lipids which are usually invoked in situations when neighboring domains are expected to phase separate because of a mismatch in bilayer thickness. Although the eutectic composition of the bilayer is composed microscopically of two distinct G(I) and G(II) gel phases, the eutectic phase is structured as a continuum, which is manifest thermodynamically by an increased phase transition cooperativity. Also, the greatest intramolecular and intermolecular disorder for C(14):C(14)PC would be expected at a binary composition for the mixture where both types of C(18):C(10)PC gel phase packing configurations contribute equally. We observe this maximum disorder in the specific acyl chain order/disorder parameters for C(14):C(14)PC at the eutectic point composition (Fig. 7). Thus, the conformational properties of the G(I) + G(II) phase may represent an entropic balance in which a high degree of two dimensional organization is assumed at the expense of a highly inter- and intramolecularly ordered chain lattice.

We observe that except near either single component limit on the phase diagram, all compositions exhibit very similar degrees of *overall* order. However, when comparing the nature of the hydrocarbon packing for each component in both the G(I) and the G(II) gel phases, it is evident that one component is more ordered, while the other component is less ordered, than their pure single component counterparts at comparable reduced temperatures. Therefore, in the region of the phase diagram corresponding to the coexistence of both G(I) and G(II) gel phases, and especially at the eutectic point, the conditions are suitable for a dynamic, fluctuating membrane state where any given C(18):C(10)PC molecule may continually interconvert between the two modes of interdigitated packing. These fluctuations may occur without any need for the membrane system to undergo a gel to fluid phase transition.

In summary, the Raman spectral data provide evidence for the existence of two modes of interdigitation for gel phase C(18):C(10)PC in the binary eutectic system composed of C(18):C(10)PC/C(14):C(14)PC. Interpretations were aided by perdeuterating the acyl chains of the C(14):C(14)PC lipid species in order to observe separately the behavior of each component within the mixture. This current investigation prepares the groundwork for successfully explaining various features involving the organization of highly asymmetric lipids existing as minor components in multicomponent bilayer systems.

References

1 Ranck, J.L., Keira, T. and Luzzati, V. (1977) Biochim. Biophys. Acta 488, 432–441.
2 Huang, C. and Mason, J.T. (1986) Biochim. Biophys. Acta 864, 423–470.
3 Slater, J.L. and Huang, C. (1988) Prog. Lipid Res. 27, 325–359.
4 Huang, C. (1990) Klin. Wochenschr. 68, 149–165.
5 Kim, J.T., Mattai, J. and Shipley, G.G. (1987) Biochemistry 26, 6599–6603.
6 Lohner, K., Schuster, A., Degovics, G., Muller, K. and Laggner, P. (1987) Chem. Phys. Lipids 44, 61–60.
7 Devlin, M.T. and Levin, I.W. (1989) Biochemistry 28, 8912–8920.
8 Mehlhorn, I.E., Florio, E., Barber, K.R., Lordo, C. and Grant, C.W.M. (1988) Biochim. Biophys. Acta 939, 151–159.
9 Florio, E., Jarrell, H., Fenske, D.B., Barber, K.R. and Grant, C.W.M. (1990) Biochim. Biophys. Acta 1025, 157–163.
10 Lin, H. and Huang, C. (1988) Biochim. Biophys. Acta 946, 178–184.
11 Huang, C., Mason, J.T. and Levin, I.W. (1983) Biochemistry 22, 2775–2780.
12 Hui, S.W., Mason, J.T. and Huang, C. (1984) Biochemistry 23, 5570–5577.
13 McIntosh, T.J., Simon, S.A., Ellington, D.C. and Porter, N.A. (1984) Biochemistry 23, 4038–4044.
14 Braganza, L.F. and Worcester, D.L. (1986) Biochemistry 25, 2591–2596.
15 Winter, R. and Pilgrim, W.C. (1989) Ber. Bunsenges. Phys. Chem. 93, 708–717.
16 Mason, J.T., Broccoli, A.V. and Huang, C. (1981) Anal. Biochem. 113, 96–101.
17 Xu, H. and Huang, C. (1987) Biochemistry 26, 1036–1043.
18 Devlin, M.T. and Levin, I.W. (1990) J. Raman Spectrosc. 21, 441–451.
19 Kirchhoff, W.H. and Levin, I.W. (1987) J. Res. Natl. Bur. Stds. 92, 113–128.
20 Levin, I.W. (1984) Adv. Infrared Raman Spectrosc. 11, 148.
21 Sisk, R.B., Wang, Z.-q., Lin, H.-n. and Huang, C. (1990) Biophys. J. 58, 777–783.
22 Mendelsohn, R., Sunder, S. and Bernstein, H.J. (1976) Biochim. Biophys. Acta 443, 613–617.
23 Levin, I.W., Thompson, T.E., Barenholz, Y. and Huang, C. (1985) Biochemistry 24, 6282–6286.
24 Janiak, M.J., Small, D.M. and Shipley, G.C. (1976) Biochemistry 14, 152–161.